

Cite this: *Mater. Adv.*, 2022,  
3, 8178

# Antimould action of Ziram and IPBC loaded in functionalised nanogels against *Aspergillus niger* and *Penicillium chrysogenum*†

Laurine Raimond,<sup>a</sup> Ahmed F. Halbus,<sup>id</sup> ab Zahraa H. Athab<sup>id</sup> ac and  
Vesselin N. Paunov<sup>id</sup> \*d

We explore the antimould action of zinc bis(dimethyldithiocarbamate) (Ziram) and 3-iodo-2-propynyl *N*-butylcarbamate (IPBC) encapsulated into nanogel particles with and without surface functionalization with a cationic polyelectrolyte, poly(diallyldimethylammonium chloride) (PDAC). The antimould nanocarriers were based on commercially available polyacrylic copolymeric nanogel. The antimould agents were loaded into the nanogel particles in their swollen state in alkaline media followed by collapsing of the nanogel particles at acidic pH. We treated *Aspergillus niger* and *Penicillium chrysogenum* cultures at different concentrations of the nanocarrier-loaded antimould agent. The effect of the surface charge of the antimould agent-loaded nanocarriers was examined in order to gain better understanding of how the electrostatic interaction of the nanocarrier with the cell walls of the mould hyphae and spores impacts its antimould action. Non-coated nanocarriers proved more efficient than PDAC-coated ones in their antimould action for both Ziram and IPBC formulations. Four different methods of application of the antimould nanocarriers were also explored. We found that the application method of the nanogel carrier is crucial for its efficiency and sustained antimould delivery. Pre-mixing the nanogel-formulated Ziram or IPBC with culture media generally produced much better antimould action. Such a strategy can potentially bypass this antimould resistance and lead to novel formulations with highly sustained antimould activity at similar concentrations of the antimould agent. These insights may lead to the development of more efficient antimould treatments at lower concentration of active agent for mould control with potentially substantial economic and environmental benefits.

Received 8th March 2022,  
Accepted 23rd August 2022

DOI: 10.1039/d2ma00271j

rsc.li/materials-advances

## 1. Introduction

Moulds are fungal species which propagate by spores and colonise various surfaces by producing multicellular hyphae filaments (hyphae) into interconnected “mycelium” networks. In addition to causing a wide range of damage in agriculture

and buildings, the growth of mould has also been associated with allergies, headaches, asthma, and other respiratory problems.<sup>1,2</sup> *P. chrysogenum* is a fungus of the *Trichocomaceae* family.<sup>3,4</sup> It can be found in temperate and subtropical regions, salted food products and outdoor environments, such as water-damaged and damp buildings. *P. chrysogenum* reproduces by spreading a dry group of spores (or conidia) from the conidiophores. These spores are carried by air currents to new colonisation sites.<sup>5–8</sup> Another common representative of moulds is *A. niger*, which is a very proliferative fungus that can be found in soil, plants, fruit, and damp indoor environments.<sup>9</sup> *A. niger* reproduces asexually with airborne spores which under suitable conditions germinate and create foot cells and more branching, with the growth of conidiophores from the foot cells.<sup>9–12</sup>

Antimould agents are biocides that can selectively kill or inhibit the growth of moulds. IPBC(3-iodo-2-propynyl *N*-butylcarbamate) is a well-known antimould agent that has been utilized for many years for a wide range of applications. Due to its limited solubility in water, it has been used in interior and

<sup>a</sup> Department of Chemistry and Biochemistry, University of Hull, Hull, HU67RX, UK<sup>b</sup> Department of Chemistry, College of Science, University of Babylon, Hilla, Iraq<sup>c</sup> Environmental Research and Studies Center, University of Babylon, Hilla, Iraq<sup>d</sup> Department of Chemistry, Nazarbayev University, Kabanbay Batyr Avenue 53,

Nur-sultan, 020000, Kazakhstan. E-mail: vesselin.paunov@nu.edu.kz

† Electronic supplementary information (ESI) available: In the enclosed electronic supplementary information (ESI) we present the following additional data: (i) solubility test of Ziram; (ii) solubility test of IPBC; (iii) zeta potential and particle hydrodynamic radius of Carbopol nanogel loaded with Ziram and IPBC; (iv) the antimould activity of Ziram and Ziram-loaded Carbopol nanogel; (v) Method 1 – antimould formulation on top of the PDA gel; (vi) Method 2 – antimould formulation in the bulk of the PDA gel; (vii) Method 3 – antimould formulation in the bulk and on the surface of the PDA gel. (viii) Summary of antimould nanogel compositions with Ziram and IPBC used. See DOI: <https://doi.org/10.1039/d2ma00271j>

exterior paints,<sup>13</sup> coatings, and cosmetics.<sup>13,14</sup> Pelto *et al.*<sup>15</sup> studied the antifungal efficiency of IPBC against *A. niger* in polymer blends. Ziram (zinc bis(dimethyldithiocarbamate)) is a biocide from the dithiocarbamate family that can inhibit fungal growth and is commonly used in formulations for agriculture, on wood and plastics and other materials. Its antifungal action is based on the chelation of Fe<sup>2+</sup> necessary for aconitase.<sup>16</sup> Crebelli *et al.*<sup>17</sup> examined Ziram's antifungal activity on nine varied species including *Aspergillus nidulans*, a fungus species closely related to *A. niger*.

In this study of antimould nanoparticle applications, we have selected *Aspergillus niger* and *Penicillium chrysogenum* as typical representatives of very widespread moulds, which are responsible for multibillion dollar damage to crops, food items and buildings on an annual basis. Both of them have high proliferation rates which renders them suitable for culturing in lab conditions and testing nanotechnology-based antimould formulations on them can also help to tackle many other representatives of the *Penicillium* and the *Aspergillus* genres of moulds and become aware of the mechanisms of their antimould resistance.

Nanogels and other nanocarriers loaded with antimicrobial agents such as berberine,<sup>40</sup> chlorhexidine<sup>25</sup> and antibiotic agents like vancomycin,<sup>32</sup> ciprofloxacin,<sup>41</sup> clindamycin,<sup>26</sup> tetracycline and lincomycin,<sup>30</sup> Penicillin G and Oxacillin<sup>27</sup> as well as combinations of clavulanic acid and amoxicillin/ticarcillin<sup>43</sup> have been systematically applied to tackle antibacterial resistance. Shellac nanocarriers loaded with amphotericin B<sup>28</sup> and fluconazole,<sup>44</sup> berberine<sup>40</sup> and chlorhexidine<sup>42</sup> have also been found effective against *Candida albicans* and other yeasts, as well as against fungal biofilms. Other nanoparticle formulations based on surface-functionalized inorganic nanoparticles of CuO,<sup>36,37</sup> ZnO,<sup>33</sup> and Mg(OH)<sub>2</sub>,<sup>31</sup> have been recently explored for antibacterial and antiyeast applications.

As many fungal species have developed a strong resistance against treatment, there has been recently considerable interest in the development of nanoformulations for encapsulating and targeted delivery of antifungal agents. These nanocarriers can release locally a high concentration of the active agent by adhering directly to the fungal cells.<sup>18,19,36–38</sup> Encapsulation of cationic actives as berberine, chlorhexidine and others, into carbomers has been found to deliver antibacterial and antifungal agents by using targeted delivery.<sup>19</sup>

Other antimould agents have also been tried with other polymers with improved antifungal activity.<sup>15</sup> De Marchi *et al.*<sup>20</sup> characterised and tested a nanocarrier with triclosan and  $\alpha$ -bisabolol against pathogenic mould strains that are resistant to triclosan. Triclosan has been encapsulated into chitosan-coated-nanocapsules containing  $\alpha$ -bisabolol as a core, for use as a potential wound dressing.<sup>20</sup> The results showed that nanoencapsulation has improved the antimicrobial activity when compared to non-encapsulated activity.<sup>20</sup> Carbomer microgels have been combined with agarose networks in a semi-interpenetrating polymer network structure to facilitate a suitable delivery system for the controlled loading and release of resveratrol.<sup>21,22</sup> Lignin nanoparticles have also been used as

nanocarriers to load antimicrobial agents.<sup>23</sup> As a result, the type of lignin used, and the presence of a cationic surface coating control the properties of the nanoparticles created.<sup>23,34</sup> Previous studies have shown that cross-linked polymer nanogels can be an effective way to encapsulate and deliver drugs.<sup>19,25</sup> Polymeric nanogels as delivery systems have been shown to have exceptional stability,<sup>26–28</sup> respond to biologically relevant stimuli, allow for additional surface functionalization with cell targeting ligands and be easy to formulate.<sup>29,30</sup>

Carbomer nanogels have been successfully used to encapsulate several cationic antibacterial and antimould agents which have good aqueous solubility.<sup>19,25,26,30</sup> Al-Awady *et al.*<sup>19,25</sup> reported encapsulation of berberine and chlorhexidine into polyacrylic nanogel particles using a swelling/deswelling technique and showed that the functionalisation of berberine-loaded-nanogel particles with a cationic polymer improved their antimicrobial activity. The cationic polymer coating can allow the control of the nanoparticle's surface charge and promote adhesion to microbial cell walls, which have a negative surface charge in aqueous media.<sup>23,24,31–33,39–41,43</sup> A more comprehensive overview on the use of nanotechnology for antimicrobial and antibiofilm applications can be found in the recent reviews of Weldrick *et al.*<sup>45</sup> and Evans *et al.*<sup>46</sup> In the present study we focus on exploring a similar idea of applying surface-coated carbomer nanogels with a payload of widely used antimould agents like Ziram and IPBC to treat mould cultures.

Here, we explore antimould agent-loaded nanogels, surface functionalised with the cationic polymer PDAC on both *P. chrysogenum* and *A. niger*. Our approach is based on encapsulating Ziram or IPBC for antimould applications by using carbomer nanogels based on a partially cross-linked polyacrylic acid co-polymer. We evaluated the stability of the Ziram- or IPBC-loaded nanogel, its encapsulation efficiency, the controlled release of encapsulated payload and the toxicity of the formed Ziram or IPBC-nanogel complexes and their surface functionalised versions. Fig. 1A describes schematically the encapsulation steps of Ziram or IPBC into the nanogel and the surface functionalisation with PDAC of the produced nanocarriers. The retention of the Ziram or IPBC in the core of the nanogel is based on electrostatic interaction with non-covalent bonding to ensure further slow release of the antimould agent upon incubation of the loaded nanogel particles with the tested mould. We also explored the effect of the ways of delivery of the nanoformulation on its antimould efficiency (Fig. 1C).

## 2. Materials and methods

### 2.1. Materials

All glassware used in this work was washed with deionized water and commercial detergent, then with absolute ethanol and rinsed with deionized water. Dettol Mould and Mildew Remover™ spray, purchased from a local supermarket, and ethanol spray were used to clean the benchtops and all working surfaces to minimize the risk of spreading of mould spores and cross-contamination. Sodium hydroxide and hydrochloric acid





(at 0.11 wt%) at pH adjusted in the range of 4.75–5.00 using an acetate buffer solution (1–2 drops) with intensive stirring. The produced cationic nanoparticles were characterized using a Zetasizer Nano ZS, (Malvern Instruments, UK).

#### 2.4. Preparation of the mould growth medium

All described experiments are conducted with this PDA media. PDA media was prepared as follows: 39 g of PDA was dissolved in 1 L of deionized water, autoclaved at 121 °C for 15 min and poured into sterile Petri dishes in a sterile field over a Bunsen burner. The dishes were half-filled with PDA media and left undisturbed until the agar solution solidifies.

#### 2.5. Seeding of the mould samples into the PDA loaded Petri dishes

Before preparing the Petri dishes with PDA, all of the hood surfaces were cleaned by spraying with ethanol. The mouths of the tubes were sterilized before and after use (using the flame of a Bunsen burner). Using a sterile micropipette, one drop of the mould suspension was transferred to the centre of a Petri dish. The lid of the Petri dish was closed and labelled with the name of the culture and the date; then a thin strip of parafilm was wrapped around the sides of the plate to cover the opening. The Petri dishes were placed in an incubator at 25 °C. After 6 days, a small amount of the grown mould was collected from the centre of the Petri dish and dispersed into a tube with autoclaved water. This suspension was used to do the experiments with these mould species, as described below.

#### 2.6. Assessment of the antimould activity of nanogel-encapsulated Ziram and IPBC towards

##### *P. chrysogenum* and *A. niger*

A series of PDA-loaded Petri dishes were used to determine the antimould activity of the Ziram- and IPBC-loaded nanogel formulations. For this purpose, 0.5 mL of the tested formulation was carefully spread on the PDA gel plate by shaking the Petri dish to disperse the fungicide across the entire gel surface. The Petri dishes were left for one hour to allow the PDA gel to absorb the liquid and then were placed vertically to eliminate any excess liquid. A dispersion of the mould spores was prepared in autoclaved water, as described in the previous section. Sterile non-treated filter paper disks were then dipped in this dispersion and further placed in the centre of each PDA gel-loaded Petri dish with the help of tweezers while taking care not to touch the surface of the agar plate. Finally, the Petri lid was closed, and the plate was labelled, including the name of the culture and the date. Petri dishes were wrapped with a thin strip of parafilm around the sides of the plates to cover the opening. The culture was put in an incubator (Stuart, Orbital Incubator, SI500), at 25 °C. Digital photographs of the PDA-gel plates were taken over a period of 5 to 7 days at the same time every day to evaluate the growth of the mould samples. These images were then analysed with the software ImageJ to measure the colony diameter size and produce a graph of the colony average diameter *versus* time.

## 3. Results and discussion

### 3.1. Characterization of the PDAC-modified Carbopol nanogels loaded with Ziram or IPBC

In order to encapsulate Ziram into the Carbopol nanogel, the antimould agent must be soluble in water, and its concentration must not exceed the solubility limit. At concentrations of Ziram in aqueous solutions above its molecular solubility limit, it turns into a colloidal suspension. This colloidal form of Ziram makes impossible its direct encapsulation from aqueous solution into the Carbopol nanogel by pH swelling/deswelling cycles.<sup>19,25</sup> We tested visually for the presence of aggregates in the Ziram solution by using a laser pointer test which allows the visual detection of the presence of these particulates for the concentration range 0.01–0.2 wt% (see Fig. S1, ESI<sup>†</sup>). The visibility of the laser beam going through the Ziram solution indicated that the solution is colloidal due to the so-called Tindal effect. Light from the laser beam gets scattered by the colloid particles of Ziram and becomes visible by the side observer, which would not be possible at concentrations where the Ziram is forming a molecular solution. One can see that Ziram forms a molecular solution in water at concentrations below 0.04 wt%. As the addition of the antimould agent into Carbopol nanogel occurs at pH 8 and at room temperature, the antimould agent must be soluble under these conditions. Therefore, for the purpose of our study we used concentrations of Ziram less than or equal to 0.02 wt% in our nanogel encapsulation protocol.

Fig. S2 (ESI<sup>†</sup>) shows that above the solubility limit of IPBC, aggregates start to be formed and the resultant IPBC particles cannot be encapsulated in the Carbopol nanogel. As the addition of the antimould agent into the Carbopol nanogel occurs at pH 8 and at room temperature, the antimould agent must be soluble under these conditions. We utilized the Tyndall effect with a laser beam test for a series of IPBC solutions of different overall concentrations, which allowed us to detect the concentration limit above which IPBC starts forming aggregates. Fig. S2 (ESI<sup>†</sup>) shows that at pH 8, IPBC solutions of concentrations from 0.005 wt% to 0.04 wt% do not scatter light and IPBC forms a molecular solution. On the contrary, above the IPBC concentration of 0.04 wt%, the IPBC solutions are colloidal. As the six IPBC solutions from 0.005 wt% to 0.04 wt% seem to meet the necessary conditions detailed before, they were used for the experiments of encapsulation within Carbopol and further coating with PDAC to induce a positive surface charge.

We studied the zeta potential and particle mean hydrodynamic diameter of the Carbopol Aqua SF1 nanogels loaded with Ziram or IPBC and then coated with PDAC. Fig. S3A (ESI<sup>†</sup>) shows that the encapsulation of Ziram into the nanogel particles following our protocol did not induce a significant variation of the zeta potential compared with the non-loaded nanogel alone. However, the coating of these nanocarriers with PDAC reversed the zeta potential from negative,  $-35 \pm 6$  mV, to positive,  $15 \pm 10$  mV. Fig. S3B (ESI<sup>†</sup>) shows that the size of the nanocarriers after the encapsulation of Ziram into the Carbopol Aqua SF1 is higher ( $140 \pm 3$  nm) than the size of the non-loaded Carbopol nanogel particles alone ( $100 \pm 2$  nm) at pH 5 where the nanogel





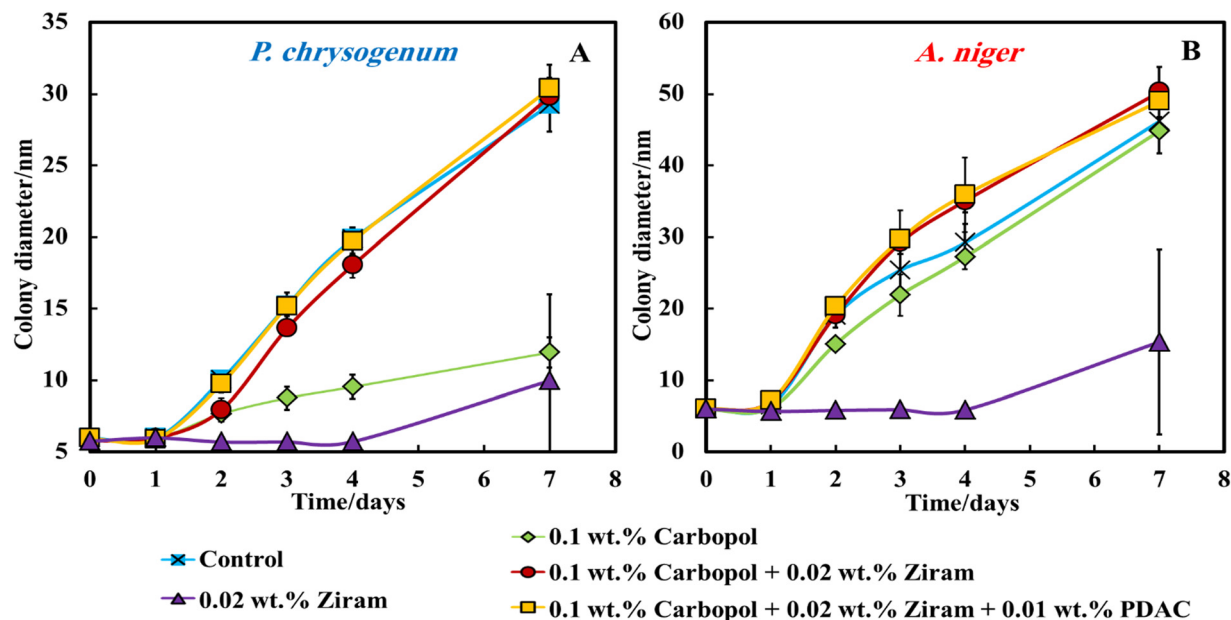


Fig. 2 The diameter growth of the *P. chrysogenum* (A) and *A. niger* (B) colony over the period of 7 days on PDA media. The PDA media has been prepared and poured into Petri dishes. Then, 0.5 mL of each formulation was added on the top of each Petri dish. Finally, a paper disk impregnated with the mould suspension was put in the centre of each Petri dish. The growth was monitored by digitally photographing the PDA gel plate every day at the same hour by measuring the average diameter of the colony. The error bars in some of the data points are within the scale of the data symbol.

is in a collapsed state. However, the average hydrodynamic diameter of these nanogel particles coated with PDAC was similar to the one of the non-coated nanogel. This is consistent with the deposition of a single layer of PDAC on the nanocarrier surface, which is known from the literature to be around 1.5 nm in thickness.<sup>34</sup> We also found that the encapsulation of IPBC into the Carbopol nanogel particles does not produce a significant change in the zeta potential compared to the Carbopol nanogel alone (Fig. S3C, ESI†). However, the coating of the nanocarriers with PDAC reverses their zeta potential from a negative ( $-40 \pm 2$  mV) to a positive value ( $20 \pm 5$  mV), *i.e.* makes them surface cationic. The PDAC coating is expected to increase the adhesion between the positively charged antimould-loaded nanocarriers and the negatively charged cell walls of the mould hyphae and spores.

Fig. S3D (ESI†) shows that the average hydrodynamic diameter of the nanocarriers after the encapsulation of IPBC into Carbopol is higher ( $140 \pm 3$  nm) than the size of the nanogel particles alone ( $100 \pm 2$  nm). The IPBC-loaded nanocarrier particle size after coating with PDAC was also similar to the size of the non-coated nanocarriers.

### 3.2. The antimould activity of Ziram and Ziram-loaded Carbopol nanogels

**3.2.1. Method 1 – antimould agent applied on the PDA gel plate surface.** We compared the antimould activity of free Ziram and Ziram-loaded Carbopol nanogels (non-coated) on the same mould cultures, *P. chrysogenum* and *A. niger* in order to determine whether the loading of Ziram within the Carbopol nanogel particles could enhance the Ziram antimould activity. Method 1 consisted of preparation of PDA media, autoclaving it,

pouring it into Petri dishes and finally, after setting adding 0.5 mL of each formulation on the top of each Petri dish. Then, a little disk of filter paper impregnated with the mould spores was placed in the centre of the Petri dish.<sup>35</sup> One can see that the nanogel alone has no effect on the mould growth. According to Fig. 2A and B, 0.02 wt% Ziram concentration suppressed the growth of both *A. niger* and *P. chrysogenum* until day 4 (purple line). After this time, the colony diameters start to increase for both kinds of moulds. Hence, the 0.02 wt% Ziram concentration marks the threshold of antimould action.

However, with this method of delivery of the Ziram formulations on the gel plate surface, we found that neither Ziram loaded into Carbopol nanogel (red line) nor Ziram loaded in Carbopol nanogel and further coated with PDAC (yellow line) seem to influence the growth of both *A. niger* and *P. chrysogenum*. Fig. S4A and B (ESI†) show that 0.05 wt% (orange line), 0.1 wt% (grey line) and 0.2 wt% (yellow line) Ziram concentration did not prevent the growth of *A. niger* and *P. chrysogenum* for the first 4 days of monitoring. In the samples treated with 0.02 wt% of free Ziram, the mould growth was suppressed until day 4 (blue line), but after that, the colony diameters started to increase for both *A. niger* and *P. chrysogenum*. We also examined the effect of the cationic polyelectrolyte PDAC on the mould growth. Fig. S4A and B (ESI†) show that the presence of PDAC at any concentration in the range 0.005–0.1 wt% does not seem to affect the mould growth.

To gain a better insight into the growth of the *A. niger* and *P. chrysogenum* samples on the PDA gel plates and to understand the reason for the lack of antimould action with nanogel-encapsulated Ziram, we imaged a cross-section of the gel with an optical microscope, as shown in Fig. 3. Fig. 3B, F, D and H show optical microscope images of *A. niger* and *P. chrysogenum*



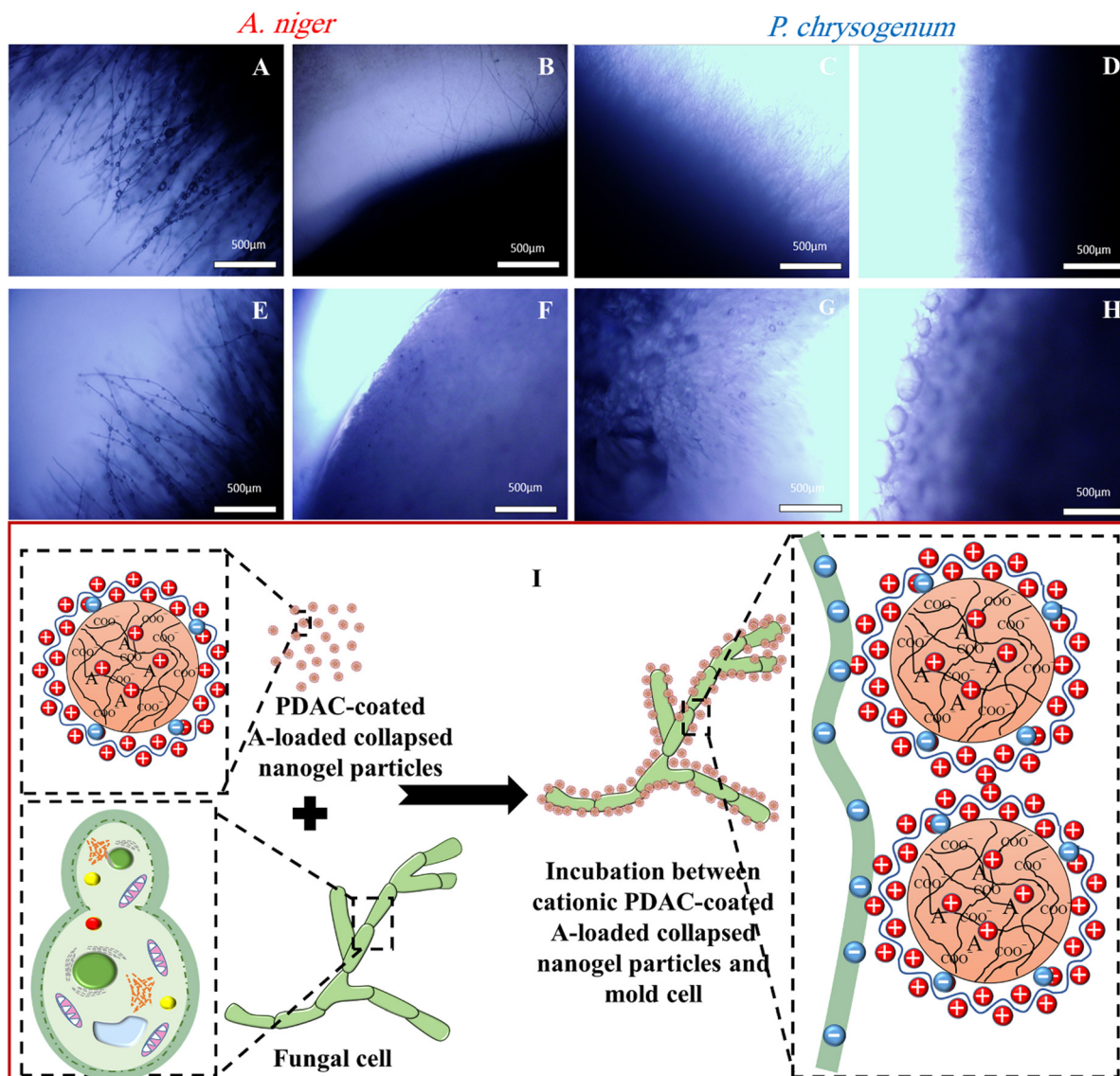


**Fig. 3** Optical microscope images of a section of the PDA media from Petri dishes of *A. niger* alone (A and E) and *A. niger* + 0.02 wt% Ziram (B and F). (A and B) were taken on the 2nd day, while (E and F) were taken on the 4th day since the inoculation of the gel plate with the mould. Optical microscope images of a section of the Petri dishes with a growing colony of *P. chrysogenum* alone (C and G) and *P. chrysogenum* + 0.02 wt% Ziram (D and H). (C and D) were taken on the 2nd day, while (G and H) were taken at the 4th day since the inoculation of the PDA gel plate with the mould. (I) The schematic of the electrostatic interaction between PDAC-coated Ziram- or IPBC-loaded Carbopol microgel particles and the outer cell membrane of mould hyphae in which the IPBC or Ziram is delivered locally on the mould cell membrane.

mould after incubation with Ziram for up to 4 days. After 2 days of culturing in Petri dishes with PDA media, both *A. niger* and *P. chrysogenum* mould hyphae begin to appear, as shown in Fig. 3A, E, C and G.

Note that both *A. niger* and *P. chrysogenum* were growing their hyphae network through the gel. This indicates that both *A. niger* and *P. chrysogenum* were propagating deeply under the surface of the PDA gel plate and thus, bypassing the antimould nanocarriers which are deposited on the gel surface. The optical microscope images in Fig. 3B, F, D and H also show that the presence of Ziram at a concentration of 0.02 wt% suppressed the growth of both *A. niger* and *P. chrysogenum* only for the first 4 days. Optical microscope images of these mould

samples on PDA gel indicate that they were growing inside the gel, which makes them even more difficult to kill by antimould formulation treatment of the surface of the gel. Indeed, by spreading their hyphae and spores inside the gel they were able to avoid the zones with antimould agent irrespective of the presence of the nanoformulation of Ziram. Hence, the mould bypasses the antimould nanocarriers by growing through the gel which effectively “filters out” the nanocarrier and offsets its action away from the hyphae. This insight led us to rethink the setting of the antimould testing method.

Therefore, in addition to the direct spreading of the tested antimould formulation on top of the PDA gel plate (Method 1), several additional settings were explored, such as (Method 2)



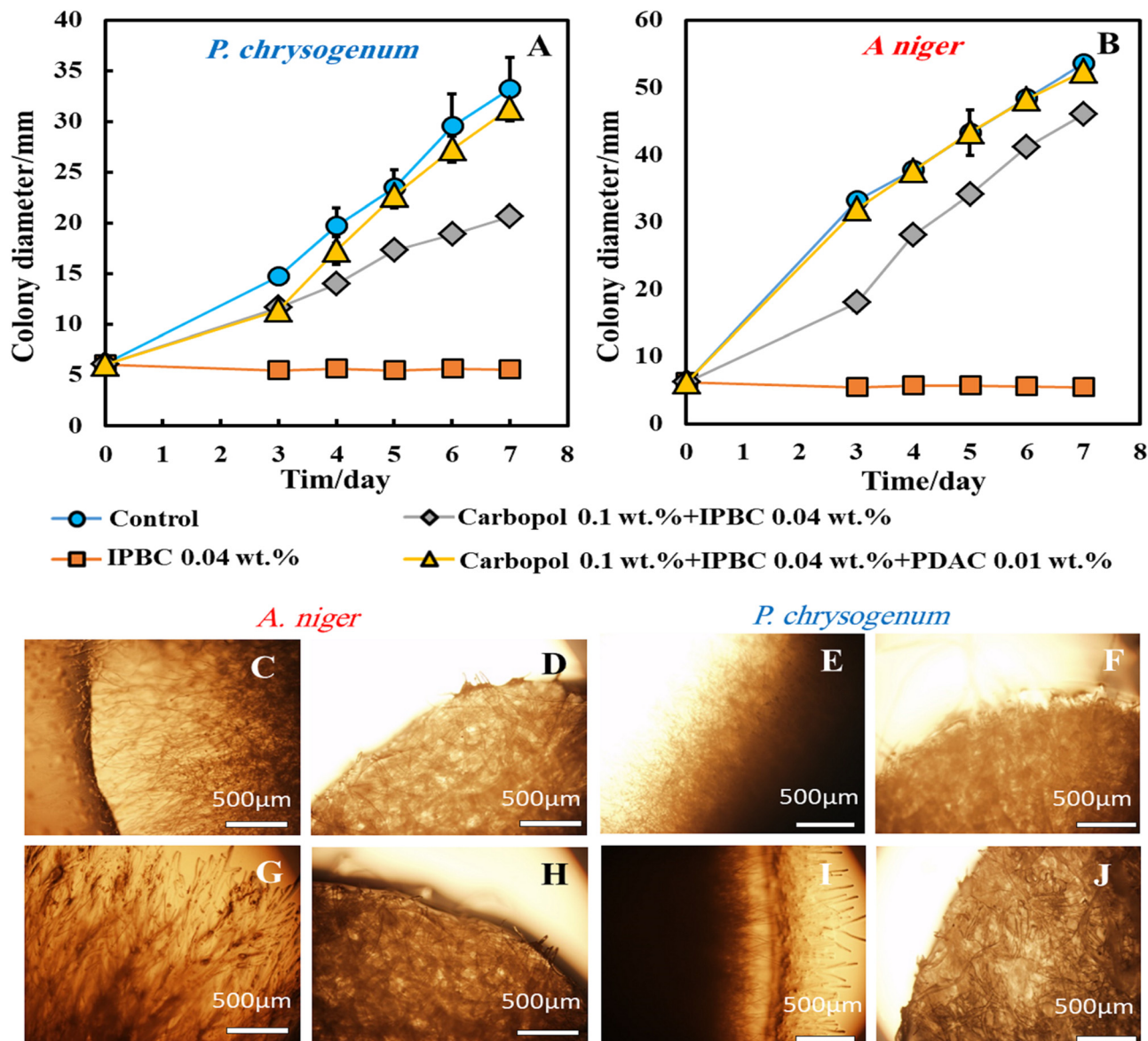


Fig. 4 The diameter of the growing *P. chrysogenum* (A) and *A. niger* (B) colony over a period of 7 days on PDA gel media. Testing Method 1 was applied and the mould growth was monitored every day at the same hour by measuring the diameter of the colony. Optical microscopy images of sections of the PDA gel from the sample of *A. niger* alone (C and G) and *A. niger* + IPBC 0.04 wt% (D and H). (C and D) were taken after 2 days, while (G and H) were taken after 4 days, respectively. Microscope images were taken of a cross-section of the PDA gel with a colony of *P. chrysogenum* alone (E and I) and *P. chrysogenum* + IPBC 0.04 wt% (F and J). (E and F) were taken after 2 days, while (I and J) were taken after 4 days. The error bars in some of the data points are within the scale of the data symbol.

mixing the antimould nanocarrier formulation with the gel media, (Method 3) mixing with the growth media and applying on top of the gel, and (Method 4) applying the antimould formulation on top of the seeding disk with the mould (see Fig. 1C). The results indicate that the threshold of the free Ziram concentration efficient to prevent the mould growth is 0.02 wt%. However, we found that electrostatic attraction between the PDAC-coated Ziram-loaded Carbopol nanogel suspension particles and the outer cell membrane of mould as schematically shown in Fig. 3I did not result in enhancement of the antimould action of Ziram. The most likely reason for this result is the inability of the nanoparticles to penetrate deeply

into the gel media and reach the hyphae, which grow underneath. However, the free Ziram solution can penetrate the PDA gel and reach the hyphae, which explains why it is active under these conditions.

### 3.3. The antimould activity of IPBC-loaded Carbopol nanogels

**3.3.1. Method 1 – antimould agent applied on the PDA gel plate surface.** The antimould activity of the IPBC-loaded Carbopol nanogels was also evaluated against both moulds (*A. niger* and *P. chrysogenum*) for a formulation of 0.04 wt% IPBC encapsulated in 0.1 wt% Carbopol nanogel, coated with





0.01 wt% PDAC. Method 1 for the application of the sample was done as described in the previous section.

Fig. 4A and B, 0.04 wt% IPBC encapsulated in 0.1 wt% Carbopol nanogel and coated with 0.01 wt% PDAC (yellow line in Fig. 4) did not have a measurable effect on the growth of both *A. niger* and *P. chrysogenum* under Method 1 of application. For these samples, the growth of both moulds was similar to the growth of the control samples. However, 0.04 wt% free IPBC aqueous solution (the orange line in Fig. 4) completely suppressed the growth of both *A. niger* and *P. chrysogenum*. This observation means that this concentration of free IPBC is high enough to inhibit the growth of both types of moulds. 0.04 wt% IPBC encapsulated in 0.1 wt% Carbopol (the grey line in Fig. 4) also has a negligible effect on their growth. This is counter-intuitive as one would expect the PDAC to amplify the action of the encapsulated IPBC. Fig. 4C, G, E and I show that the *A. niger* and *P. chrysogenum* mould in the control sample grows faster than in other Petri dishes treated with 0.04 wt% free IPBC. The control sample grew after day 2, while mould samples treated with the 0.04 wt% IPBC did not grow at all, *i.e.* the sample diameter stayed at 5 mm. After 2 days of culturing on the PDA gel media, both *A. niger* and *P. chrysogenum* mould growth begin to appear, as shown in Fig. 4C, G, E and I. Recalling that both moulds were growing through the gel, this is not surprising as it allows them to avoid the antimould action of the IPBC nanocarriers which has been placed on the top of the gel plate. It was found that the presence of IPBC at the concentration of 0.04 wt% displayed a strong antimould activity against both *A. niger* and *P. chrysogenum* (Fig. 4D, H, F and J).

Since the nanocarriers cannot penetrate through the PDA gel, the concentration of IPBC that reaches the hyphae is much lower, which prevents the antimould agent from reaching the growing mould hyphae under the gel at high enough concentrations.

Fig. S5 (ESI<sup>†</sup>) shows that the mould in the control sample grows faster than other Petri dishes treated with the free IPBC, IPBC encapsulated in 0.1 wt% Carbopol nanogel, and IPBC encapsulated in 0.1 wt% Carbopol nanogel coated with 0.01 wt% PDAC over the period of 7 days. Typically, the mould colony grew from a diameter of 5 mm until it reached 53 mm for *A. niger* and 33 mm for *P. chrysogenum* after day 7, while mould samples treated with the free IPBC-based antimould formulations did not grow at all and the sample diameter stayed at 5 mm. It was found that free IPBC on its own had a significant antimould activity against *A. niger* and *P. chrysogenum* at concentrations of 0.04 wt% and suppressed the mould growth. Like the experiments with Ziram formulations, we also did several different settings with Methods 2 and 3 by putting the antimould nanocarrier solution inside and on top of the PDA gel instead of on the top of the gel only (Method 1).

**3.3.2. Method 2 – mixing of the antimould formulation with the growth medium.** In this method, we studied the antimould properties of the IPBC encapsulated in Carbopol nanogel coated with PDAC against *A. niger* and *P. chrysogenum* by mixing them with the liquid PDA medium at 40 °C before the gel sets on the plate at 25 °C. The rationale behind this is that the hyphae of both kinds of mould grow through the PDA gel and propagate, which leaves the possibility for the hyphae to bypass any antimould nanocarriers in the suspension

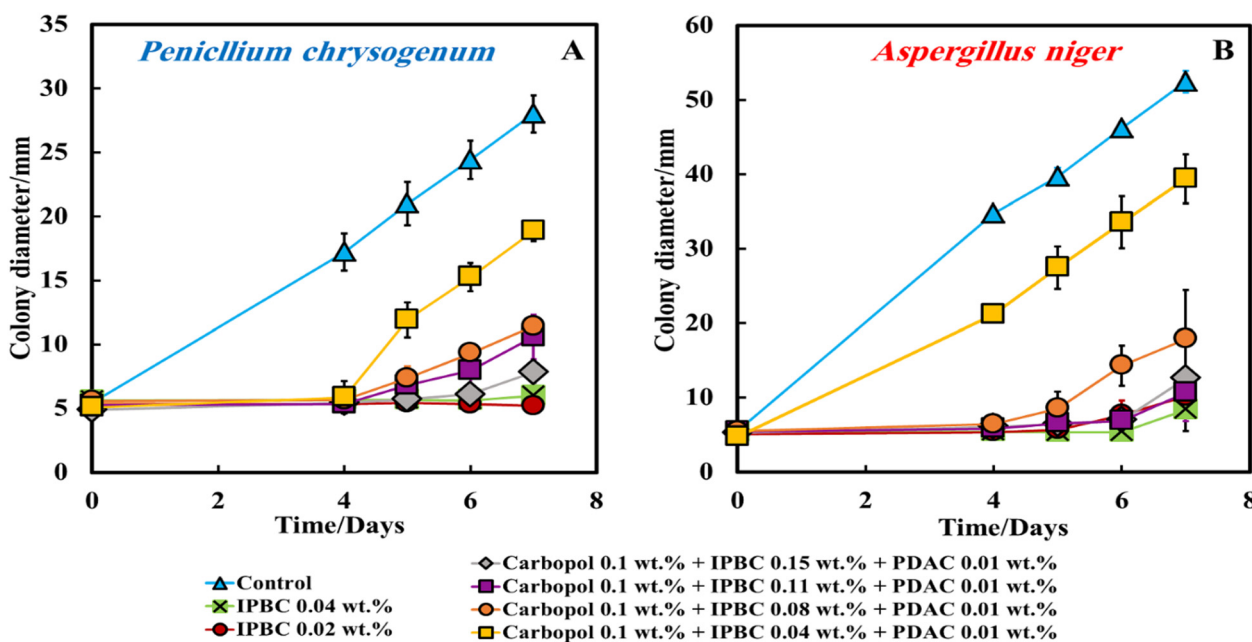


Fig. 5 The colony diameter growth of *P. chrysogenum* (A) and *A. niger* (B) over the period of 7 days on PDA media. The media was prepared, autoclaved and then the 4 different formulations of nanocarrier were mixed with the growth medium. Method 2 consisted in preparing PDA media, autoclaving it, cooling to 40 °C and then mixing it with the antimould nanocarrier suspension, and finally pouring it into each Petri dish to quickly set at room temperature. Then, a sterile filter paper disk impregnated with the mould suspension was put in the centre of each Petri dish. The error bars in some of the data points are within the scale of the data symbol.





formulation when it is applied only on the surface of the PDA gel plate. Method 2 consisted in preparing PDA media, autoclaving it, and then mixing it with a fixed aliquot of the antimould nanocarrier suspension at a room temperature just before gelling, and finally pouring it into each Petri dish. Then, a 5 mm sterile disk of filter paper impregnated with the mould suspension was carefully placed in the centre of each Petri dish.<sup>35</sup> Every formulation of IPBC encapsulated in Carbopol nanogel coated with PDAC (yellow, orange, purple and grey lines) made according to Method 2, suppressed the growth of both *A. niger* and *P. chrysogenum* for up to 4 days. After that, the colony diameter started to increase for both kinds of moulds. This set of experiments, which is incorporating the nanocarrier suspension inside the culture media, prevented the mould from bypassing the antimould agent. Fig. 5A and B show the results of the antimould tests of both moulds species where the control samples of untreated mould were compared with the ones treated with free IPBC, IPBC encapsulated in Carbopol nanogel and IPBC encapsulated in Carbopol nanogel coated with PDAC.

Note that when dispersed in the gel matrix, the free IPBC also showed an antimould effect on *A. niger* and *P. chrysogenum*.

We found that at a concentration of 0.04 wt% free IPBC, the growth rate of *A. niger* and *P. chrysogenum* reduced several-fold compared with the control samples of the untreated mould. A strong impact of the free IPBC on *A. niger* and *P. chrysogenum* was observed after 5 days of incubation at 25 °C.

According to Fig. 5A and B, 0.04 wt% IPBC solution (the green line) totally suppressed the growth of *A. niger* and *P. chrysogenum* for 7 days. However, 0.02 wt% free IPBC solution (red line) prevented the growth of these moulds until day 6 since inoculation. The concentration of 0.04 wt% of free IPBC seems to be the threshold. Fig. 5A and B show that without an antimould agent, the mould has a growth diameter of 53 mm for *A. niger* and 28 mm for *P. chrysogenum* after 7 days, while it was found that different formulations of antimould nanocarriers have a high antimould activity against both *A. niger* and *P. chrysogenum*. This shows that when dispersed throughout the matrix of the growth media, the antimould nanocarriers effectively kill the spreading mould and suppress its growth (Fig. S6, ESI†).

The experimental data show that by increasing the IPBC content encapsulated in the nanogel from 0.04 wt% to 0.15 wt% the antimould activity increases strongly and becomes

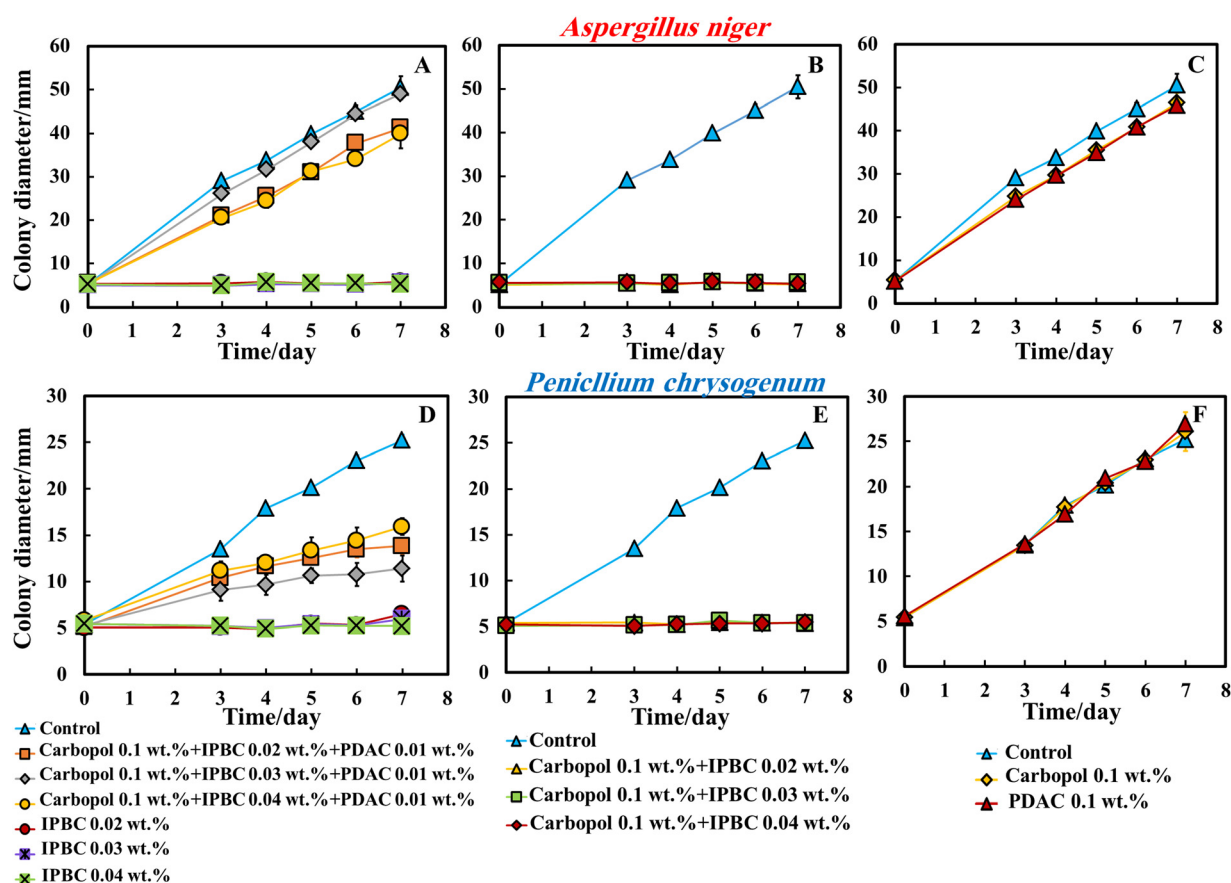


Fig. 6 The average colony growth diameter of *A. niger* (A–C) and *P. chrysogenum* (D–F) as a function of time. The control samples of both moulds were kept under the same conditions without treatment with antimould agent for the same period and the suspensions of IPBC encapsulated in 0.1 wt% Carbopol Aqua SF1 nanogel and coated with 0.01 wt% PDAC at various IPBC concentrations. Method 3 consisted of preparing PDA media, autoclaving it, cooling to room temperature, and then mixing it with a nanocarrier suspension, pouring it into each Petri dish, and finally after the agar sets, spreading 0.5 mL of each formulation on the top of the gel. Then, a sterile filter paper disk impregnated with the mould has been put in the centre of each Petri dish. The error bars in some of the data points are within the scale of the data symbol.



comparable with the free IPBC formulation at 0.04 wt%. The IPBC encapsulation however provides a sustained release of IPBC over the period of 7 days against both *A. niger* and *P. chrysogenum* even for very short times. We did not see an enhancement of the IPBC action with the nanocarrier-encapsulated IPBC as it releases lower concentration of IPBC over a longer period. The PDAC coating also proved of no benefit to the antimould action as the nanocarriers get trapped in the gel and cannot freely migrate towards the growing hyphae. One would expect such enhancement to occur if the PDAC can promote adhesion of the nanocarrier to the hyphae and the spores of the mould. However, here the effective immobilization of the nanocarrier particles within the gel media prevents them from achieving this and to adhere on the cell walls where they could release more concentrated IPBC causing mould death.<sup>19,25</sup>

Method 2 as an application of the nanoformulation gave superior results compared with Method 1, described in the previous section.

### 3.3.3. Method 3 – antimould agent (nanocarriers suspensions) in the bulk and the surface of the growth media.

The technique used in Method 2 was followed here as outlined above with mixing of the antimould agent (nanocarriers suspensions) with the PDA media. To further strengthen the antimould action, we mixed the antimould nanogel particle suspension with the PDA media above its gelling point (in liquid state) and after its gelling we also added the same antimould agent on the top of the gelled medium, similarly as described in Method 1. Method 3 consisted of preparing PDA media, autoclaving it, and then mixing it with the antimould nanocarrier suspension, pouring it into each Petri dish, and finally after the agar sets, spreading 0.50 mL of each formulation on the top of the PDA gel plate. Then, a 5 mm filter paper disk with the mould suspension was put in the centre of each Petri dish.<sup>35</sup> Hence in Method 3, we had antimould agent both in the bulk of the growth media and on its surface.

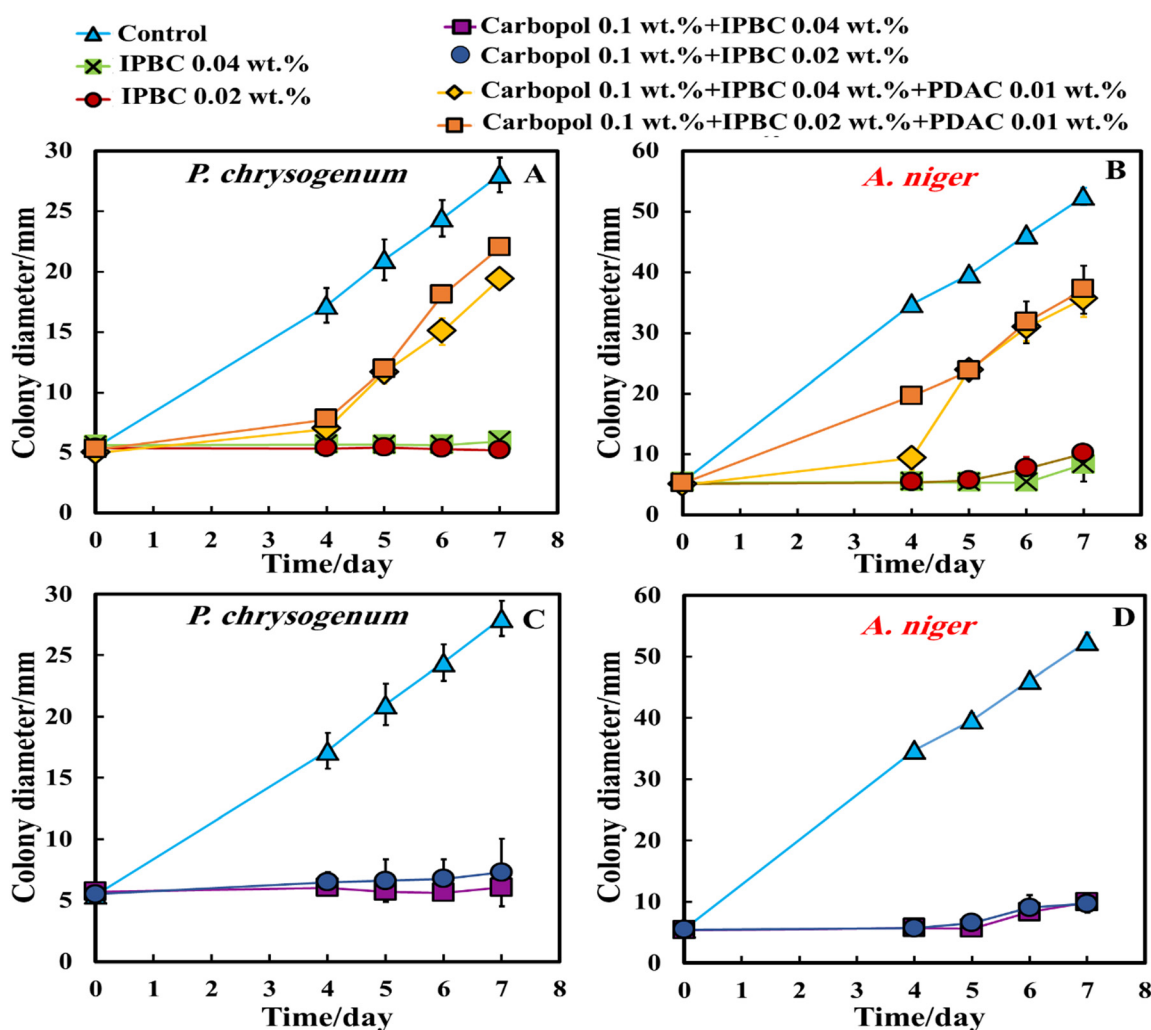


Fig. 7 The average colony growth diameter of *P. chrysogenum* (A and C) and *A. niger* (B and D) as a function of time. The control samples of both types of mould were kept under the same conditions without treatment with antimould agent for the same period and the suspensions of IPBC encapsulated in 0.1 wt% Carbopol Aqua SF1 nanogel coated with 0.01 wt% PDAC at various IPBC concentrations. The antimould formulation was applied by using Method 4, i.e. directly on the top of each paper disk containing the mould spores. The error bars in some of the data points are within the scale of the data symbol. The error bars in some of the data points are within the scale of the data symbol.



Fig. 6A and 6D show the antimould effect of the suspensions of IPBC encapsulated in 0.1 wt% Carbopol nanogel coated with 0.01 wt% PDAC at various IPBC concentrations on *A. niger* and *P. chrysogenum* at various times since inoculation. Fig. 6A indicates that the growth diameter of the *A. niger* spot in the presence of the antimould nanocarrier suspension agent was found to be around 5 mm compared with the untreated sample of 53 mm after 7 days. These results also show that the 0.04 wt% IPBC encapsulated in 0.1 wt% Carbopol nanogel coated with 0.01 wt% PDAC has an impact on mould – see Fig. S7 (ESI<sup>†</sup>). Control samples of *A. niger* and *P. chrysogenum* were kept under the same conditions without treatment with antimould agent for the same period.

Although there is a substantial effect from the cationic nanocarriers, their antimould action was found to be lower than the equivalent concentration of free IPBC.

In order to examine the effect of the PDAC coating, we also did the same experiment with IPBC without PDAC coating. Surprisingly, the data in Fig. 6B and E indicate that the 0.02–0.04 wt% of IPBC loaded in Carbopol nanogel without coating with PDAC had an extremely strong effect on *A. niger* and *P. chrysogenum*, suppressing the growth along all 7 days since

inoculation for both types of mould. As it can clearly be seen, on day 7 the growth diameter of *P. chrysogenum* was around 5.5 mm compared with the control samples of diameter 28 mm. Since in both Methods 2 and 3, the antimould nanocarrier suspension formulation is applied in the bulk of the PDA-gel, the hyphae of both *A. niger* and *P. chrysogenum* cannot grow effectively within it, which has a strong influence on their propagation – the latter was well suppressed for all formulations for over 7 days.

This was an unexpected result as it was anticipated that the negative charge of the nanogel particles loaded with IPBC will keep them apart from the mould hyphae surface within the gel but their strong antimould effect (Fig. 6B and E) came opposite to the expectations since the cell walls of *A. niger* and *P. chrysogenum* are both negatively charged. It also shows that the moulds respond differently to cationic nanocarriers compared to bacteria and yeast.<sup>28,30</sup> One possible explanation is that the non-coated IPBC nanocarriers have some mobility through the PDA gel and do not get attached to negatively charged groups on the gel network. Fig. 6C and F represent a comparison between the antimould action of different concentrations of IPBC encapsulated in 0.1 wt% Carbopol nanogel.

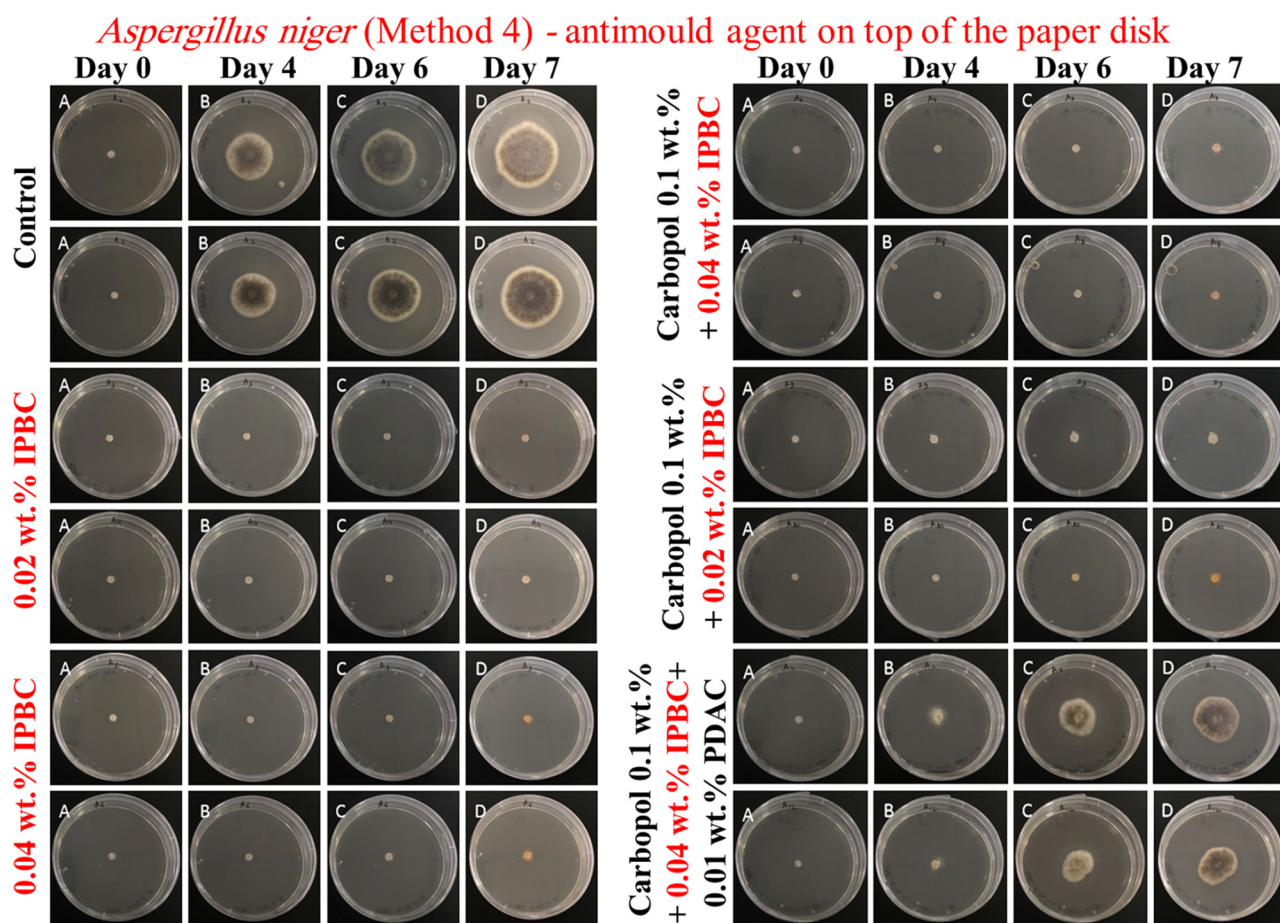


Fig. 8 Digital photographs of the PGA-gel plates containing *A. niger* sample seeded in the centre and treated with antimould agent (free IPBC and IPBC encapsulated in 0.1 wt% Carbopol nanogel and coated with 0.01 wt% PDAC) at various IPBC concentrations. The antimould formulation was applied by using Method 4, i.e. directly on the top of each paper disk containing the mould spores.





Control samples of *A. niger* and *P. chrysogenum* were kept under the same conditions without treatment with antimould agent for the same period. The control as well as the non-loaded 0.1 wt% Carbopol nanogel and the free PDAC at 0.1 wt% samples had no measurable effect on the growth rate of *P. chrysogenum* and only minor impact on the growth of *A. niger* (Fig. 6C and F).

Fig. S7 (ESI<sup>†</sup>) shows that IPBC encapsulated in 0.1 wt% Carbopol nanogels has an extremely strong impact on *A. niger* and *P. chrysogenum*. The growth rate of the mould decreased after day 7. On day 7 the growth diameter was around 5 mm compared with the control samples of diameter 53 mm for *A. niger* and 28 mm for *P. chrysogenum*.

**3.3.4. Method 4 – antimould (nanocarriers suspensions) agent applied on the paper disc with mould seeded on a PDA-plate.** The antimould action of free IPBC and its nanocarrier suspensions (0.1 wt% Carbopol nanogel coated with 0.01 wt% PDAC at various IPBC concentrations) were also studied against both moulds (*A. niger* and *P. chrysogenum*) at overall 0.02 wt% IPBC and 0.04 wt% IPBC concentration of the antimould agent. In this way, we deposited paper discs with the mould suspension also impregnated with the antimould agent. Method 4 consisted in preparing PDA media, autoclaving it and pouring it

into each Petri dish. A filter paper disk impregnated with mould spores was placed in the centre of each Petri dish. Finally, 0.5 mL of each formulation was added directly on the top of each paper disk containing the mould spores.<sup>35</sup> It was found that the free IPBC and IPBC encapsulated in 0.1 wt% Carbopol nanogel coated with 0.01 wt% PDAC at various IPBC concentrations showed a strong antimould activity against both *A. niger* and *P. chrysogenum* (Fig. 7A–D) after day 4. Fig. 7 shows that without an antimould agent (free IPBC and IPBC encapsulated in Carbopol nanogel coated with PDAC), the mould has a growth diameter of 35 mm for *A. niger* and 17 mm for *P. chrysogenum* after 4 days, while in the presence of antimould agent (0.02 wt% IPBC and 0.04 wt% IPBC concentration) the mould did not grow with the growth diameter staying at 5 mm (within the size of the paper disc).

According to Fig. 7A–D, all formulations of IPBC-loaded nanogel particles coated with PDAC applied using Method 4 (the yellow and orange lines) strictly inhibited the growth of *A. niger* and *P. chrysogenum* for up to 4 days, but after that the colony diameter increases suddenly. The goal of setting the experiment in Method 4, by placing the nanocarrier formulation on the paper disk containing the mould spores, was to kill

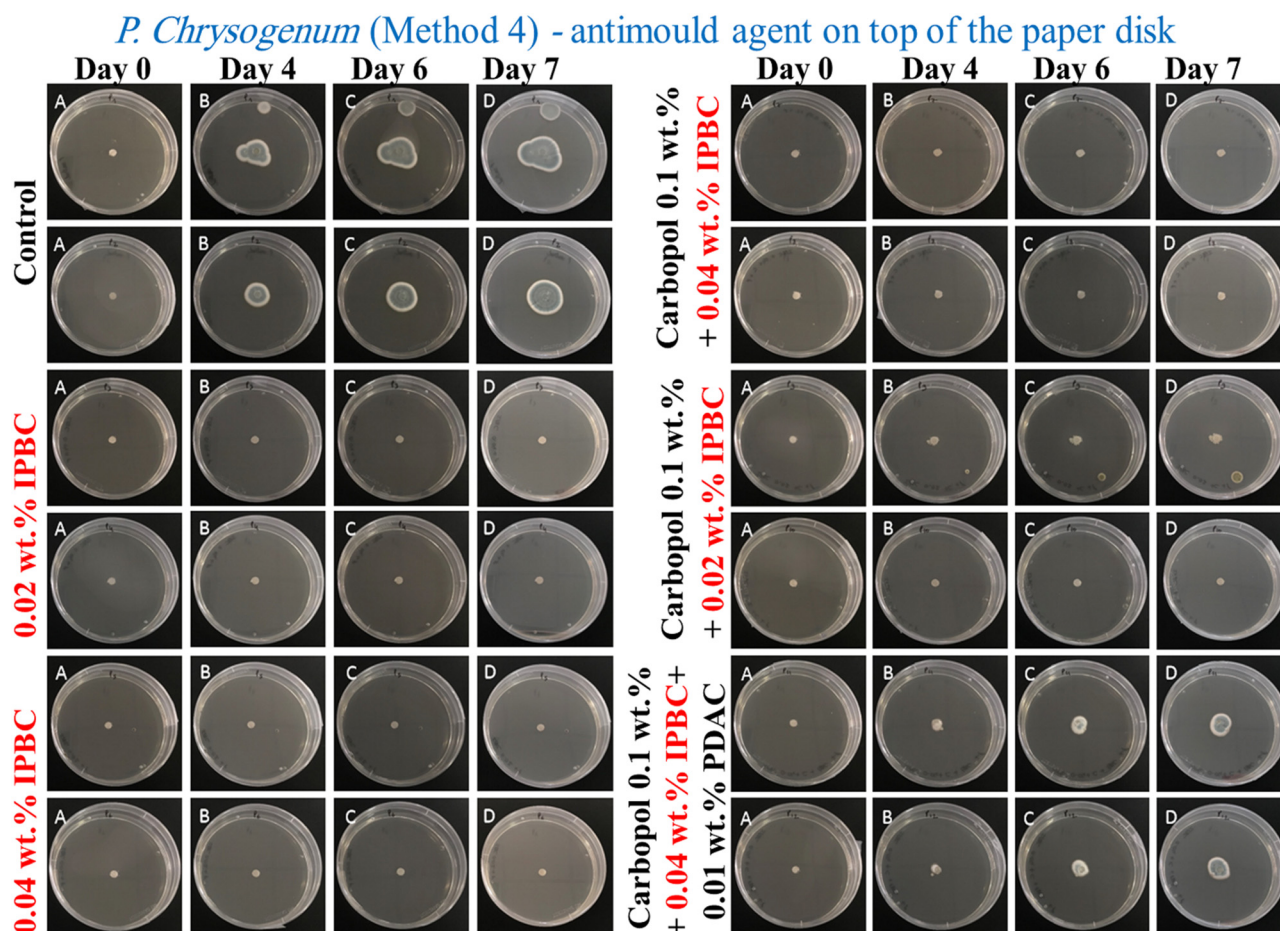


Fig. 9 Digital photographs of the PGA-gel plates containing *A. niger* spore samples seeded in the centre and treated with antimould agent (free IPBC and IPBC encapsulated in 0.1 wt% Carbopol nanogel and coated with 0.01 wt% PDAC) at various IPBC concentrations. The antimould formulation was applied by using Method 4, *i.e.* directly on the top of each paper disk containing the mould spores.



the mould spores before they can develop and propagate their hyphae through the gel.<sup>35</sup> It can be seen that the PDAC-coated IPBC-loaded Carbopol nanogel suspensions had a strong antimould impact threshold concentration of 0.04 wt% IPBC and reduced the growth of *A. niger* and *P. chrysogenum* after 4 days (Fig. 7A and B).

The same experiment was repeated with *P. chrysogenum* and *A. niger* to check if the IPBC-loaded Carbopol nanogel suspension is also a good antimould agent across various mould species (Fig. 7C and D). The control sample of the mould was kept under the same conditions without treatment with the antimould agent for the same period. In controls, the mould colony grew after day 4 to an average diameter of 17 mm for *P. chrysogenum* and 35 mm for *A. niger*, respectively. It was found that the growth rate of the mould reduced significantly compared with the control (Fig. 8 and 9). The data in Fig. 8 and 9 show that the growth spot did not change significantly from days 0 to 7 apart from the control. All tested IPBC-loaded Carbopol nanogel suspension concentrations used seem effective in subduing the mould growth. However, the PDAC-coated IPBC nanocarriers proved to be less efficient in suppressing the mould growth than free IPBC at equivalent overall concentration. Furthermore, the results show that free IPBC solutions in the concentration range 0.02–0.04 wt% have similar efficiency for both molds in their antimould action compared with the equivalent amount of IPBC-loaded Carbopol nanogel suspensions. This may potentially be explained by the fact that the IPBC-loaded Carbopol nanogel suspensions sustain the release of their payload over a long period of time, which allows the concentration of the free IPBC in their formulation to be maintained over the testing period in aqueous media.<sup>19,25</sup> In Table S1 (ESI<sup>†</sup>) we have presented the nanogel compositions with an optimal antimould effect in the table below for *P. chrysogenum* and *A. niger* and the Carbopol-loaded with Ziram- and IPBC with and without coating with PDAC.

## 4. Conclusions

We have developed a novel surface functionalized nanocarrier for Ziram or IPBC based on lightly cross-linked acrylate copolymer nanogel particles (Carbopol Aqua SF1). This nanocarrier was additionally functionalised by surface coating with the cationic polyelectrolyte PDAC. Ziram or IPBC-loaded nanogels were characterized by their particle size and zeta potential and their antimould activity has been examined on *A. niger* and *P. chrysogenum* with and without coating with PDAC. Both moulds were cultured on PDA gel plates with four different methods for application of the antimould formulation: (i) on the PDA gel surface; (ii) mixing with the PDA media; (iii) combination of (i) and (ii), and (iv) on top of the mould seeding disk. The obtained results provided insights into the ways the mould propagates through the media by bypassing the action of the antimould nanocarrier and the challenges in overcoming these by changing the application method. Our results showed that the encapsulation of IPBC into Carbopol and the coating of

these entities with PDAC did not enhance the antimould action as reported in antibacterial studies in the literature, although methods (iii) and (iv) can increase its antimould efficiency. Microscope images of these moulds on PDA gel showed that the mould hyphae were growing inside the gel, which makes them even more difficult to kill by antimould nanoformulation treatment of the gel surface. Indeed, by spreading their hyphae and spores inside the gel they were able to avoid the zones with antimould agent. Therefore, pre-mixing the nanogel-formulated Ziram or IPBC with PDA media generally produced much better antimould action. The results show that the threshold IPBC concentration efficient to prevent the growth of mould is 0.04 wt%. The experiment which had shown the best result is by method (iii) which involved putting the nanocarrier suspension inside the gel and on top of it. This prevented the mould from bypassing the antimould agent either on the top of the gel or inside the gel. Surprisingly, non-coated IPBC-loaded nanogels show superior antimould performance than the PDAC-coated nanogels, combined with sustained release of the antimould agent. Encapsulation in nanogel carriers can be potentially applied to sustain the antimould activity for a range of low-molecular weight antimould agents.

## Author contributions

VNP envisaged the idea for the project, provided methodology, resources and funding, and supervised the project team. AFH co-supervised LR and ZHA and provided technical advice. LR worked on the mould culturing, preparation of the antimould nanocarriers and experiments with them. LR and ZHA prepared the draft manuscript which was then co-edited and completed through contributions of all authors. All authors have given approval to the final version of the manuscript.

## Conflicts of interest

There are no conflicts to declare.

## Acknowledgements

A. F. H. thanks the Iraqi Government, the Higher Committee for Education Development of Iraq and the University of Babylon, Iraq for the financial support for his PhD study during the work on this project. L. R. acknowledges Ecole Supérieure de Chimie Organique et Minérale (ESCOM) for the opportunity to complete this work and the support from the ERASMUS+ mobility grant.

## References

- 1 J. Singh, Toxic moulds and indoor air quality, *Indoor Built Environ.*, 2005, **14**, 3–4, DOI: [10.1177/1420326X05054015](https://doi.org/10.1177/1420326X05054015).



- 2 D. W. Li and C. S. Yang, Fungal contamination as a major contributor to sick building syndrome, *Adv. Appl. Microbiol.*, 2004, **55**, 31–112, DOI: [10.1016/S0065-2164\(04\)55002-5](https://doi.org/10.1016/S0065-2164(04)55002-5).
- 3 C. Thom, Cultural studies of species of *Penicillium*, *Bur. Anim. Ind.*, 1910, **118**, 1910.
- 4 A. Fleming, On the antibacterial action of cultures of a penicillium, with special reference to their use in the isolation of *B. influenzae*, *Br. J. Exp. Pathol.*, 1929, **10**, 226–236.
- 5 N. Lattab, S. Kalai, M. Bensoussan and P. Dantigny, Effect of storage conditions (relative humidity, duration, and temperature) on the germination time of *Aspergillus carbonarius* and *Penicillium chrysogenum*, *Int. J. Food Microbiol.*, 2012, **160**, 80–84, DOI: [10.1016/j.ijfoodmicro.2012.09.020](https://doi.org/10.1016/j.ijfoodmicro.2012.09.020).
- 6 S. Y. Tan and Y. Tatsumura, Alexander Fleming (1881–1955): discoverer of penicillin, *Singapore Med. J.*, 2015, **56**, 366–367, DOI: [10.11622/smedj.2015105](https://doi.org/10.11622/smedj.2015105).
- 7 A. M. Soliman, W. Abdel-Latif, I. H. Shehata, A. Fouda, A. M. Abdo and Y. M. Ahmed, Green approach to overcome the resistance pattern of *Candida* spp. using biosynthesized silver nanoparticles fabricated by *Penicillium chrysogenum* F9, *Biol. Trace Elem. Res.*, 2021, **199**, 800–811, DOI: [10.1007/s12011-020-02188-7](https://doi.org/10.1007/s12011-020-02188-7).
- 8 Y. Li, M. Jiao, Y. Li, Y. Zhong, X. Li, Z. Chen, S. Chen and J. Wang, *Penicillium chrysogenum* polypeptide extract protects tobacco plants from tobacco mosaic virus infection through modulation of ABA biosynthesis and callose priming, *J. Exp. Bot.*, 2021, **72**, 3526–3539, DOI: [10.1093/jxb/erab102](https://doi.org/10.1093/jxb/erab102).
- 9 Y. Sathishkumar, N. Velmurugan, H. M. Lee, K. Rajagopal, C. K. Im and Y. S. Lee, Effect of low shear modeled microgravity on phenotypic and central chitin metabolism in the filamentous fungi *Aspergillus niger* and *Penicillium chrysogenum*, *Antonie Van Leeuwenhoek*, 2014, **106**, 197–209, DOI: [10.1007/s10482-014-0181-9](https://doi.org/10.1007/s10482-014-0181-9).
- 10 Y. Ma, T.-J. Ling, X.-Q. Su, B. Jiang, B. Nian, L.-J. Chen, M. L. Liu, Z.-A. Zhang, D.-P. Wang, Y.-Y. Mu, W.-W. Jiao, Q.-T. Liu, Y.-H. Pan and M. Zhao, Integrated proteomics and metabolomics analysis of tea leaves fermented by *Aspergillus niger*, *Aspergillus tamarii* and *Aspergillus fumigatus*, *Food Chem.*, 2021, **334**, 127560, DOI: [10.1016/j.foodchem.2020.127560](https://doi.org/10.1016/j.foodchem.2020.127560).
- 11 J. S. Poulsen, A. M. Madsen, J. K. White and J. L. Nielsen, Physiological responses of *Aspergillus niger* challenged with itraconazole. Antimicrobial agents and chemotherapy, *Antimicrob. Agents Chemother.*, 2021, **65**, e02549-20, DOI: [10.1128/AAC.02549-20](https://doi.org/10.1128/AAC.02549-20).
- 12 B. Jiang, M. Wang, X. Wang, S. Wu, D. Li, C. Liu, Z. Feng and J. Li, Effective separation of prolyl endopeptidase from *Aspergillus Niger* by aqueous two phase system and its characterization and application, *Int. J. Biol. Macromol.*, 2021, **169**, 384–395, DOI: [10.1016/j.ijbiomac.2020.12.120](https://doi.org/10.1016/j.ijbiomac.2020.12.120).
- 13 R. S. Lanigan, Final report on the safety assessment of iodopropynyl butylcarbamate (IPBC), *Int. J. Toxicol.*, 1998, **17**, 1–37, DOI: [10.1177/109158189801700503](https://doi.org/10.1177/109158189801700503).
- 14 S. Badreshia and J. G. Marks Jr, Iodopropynyl butylcarbamate, *Am. J. Contact Dermat.*, 2002, **13**, 77–79, DOI: [10.1053/ajcd.2002.30728](https://doi.org/10.1053/ajcd.2002.30728).
- 15 J. M. Pelto, S. Virtanen, T. Munter, J. Larismaa, S. Jämsä and J. Nikkola, Encapsulation of 3-iodo-2-propynyl N-butylcarbamate (IPBC) in polystyrene-polycaprolactone (PS/PCL) blends, *J. Microencapsul.*, 2014, **31**, 415–421, DOI: [10.3109/02652048.2013.843599](https://doi.org/10.3109/02652048.2013.843599).
- 16 T. S. Thind and D. W. Hollomon, Thiocarbamate fungicides: Reliable tools in resistance management and future outlook, *Pest Manag. Sci.*, 2018, **74**, 1547–1551, DOI: [10.1002/ps.4844](https://doi.org/10.1002/ps.4844).
- 17 R. Crebelli, A. Zijno, L. Conti, B. Crochi, P. Leopardi, F. Marcon, L. Renzi and A. Carere, Further in vitro and in vivo mutagenicity assays with thiram and ziram fungicides: bacterial reversion assays and mouse micronucleus test, *Teratog. Carcinog. Mutagen.*, 1992, **12**, 97–112, DOI: [10.1002/tcm.1770120302](https://doi.org/10.1002/tcm.1770120302).
- 18 J. A. Lucas, N. J. Hawkins and B. A. Fraaije, The evolution of fungicide resistance, *Adv. Appl. Microbiol.*, 2015, **90**, 29–92, DOI: [10.1016/bs.aambs.2014.09.001](https://doi.org/10.1016/bs.aambs.2014.09.001).
- 19 M. J. Al-Awady, A. Fauchet, G. M. Greenway and V. N. Paunov, Enhanced antimicrobial effect of berberine in nanogel carriers with cationic surface functionality, *J. Mater. Chem. B*, 2017, **5**, 7885–7897, DOI: [10.1039/C7TB02262J](https://doi.org/10.1039/C7TB02262J).
- 20 J. G. B. De Marchi, D. S. Jornada, F. K. Silva, A. L. Freitas, A. M. Fuentefria, A. R. Pohlmann and S. S. Guterres, Triclosan resistance reversion by encapsulation in chitosan-coated-nanocapsule containing  $\alpha$ -bisabolol as core: development of wound dressing, *Int. J. Nanomed.*, 2017, **12**, 7855, DOI: [10.2147/IJN.S143324](https://doi.org/10.2147/IJN.S143324).
- 21 M. Tunesi, E. Prina, F. Munarin, S. Rodilossi, D. Albani, P. Petrini and C. Giordano, Cross-linked poly (acrylic acids) microgels and agarose as semi-interpenetrating networks for resveratrol release, *J. Mater. Sci. Mater. Med.*, 2015, **26**, 5, DOI: [10.1007/s10856-014-5328-8](https://doi.org/10.1007/s10856-014-5328-8).
- 22 H. Es-Haghi, H. Bouhendi, G. Bagheri-Marandi, M. J. Zohurian-Mehr and K. Kabiry, Cross-linked poly (acrylic acid) microgels from precipitation polymerization, *Polym. Plast. Technol. Eng.*, 2010, **49**, 1257–1264, DOI: [10.1080/03602559.2010.496421](https://doi.org/10.1080/03602559.2010.496421).
- 23 A. P. Richter, B. Bharti, H. B. Armstrong, J. S. Brown, D. Plemmons, V. N. Paunov, S. D. Stoyanov and O. D. Velev, Synthesis and characterization of biodegradable lignin nanoparticles with tunable surface properties, *Langmuir*, 2016, **32**, 6468–6477, DOI: [10.1021/acs.langmuir.6b01088](https://doi.org/10.1021/acs.langmuir.6b01088).
- 24 N. Alipoormazandarani, T. Benselfelt, L. Wang, X. Wang, C. Xu, L. Wågberg, S. Willför and P. Fatehi, Functional Lignin Nanoparticles with Tunable Size and Surface Properties: Fabrication, Characterization, and Use in Layer-by-Layer Assembly, *ACS Appl. Mater. Interf.*, 2021, **13**, 26308–26317, DOI: [10.1021/acsami.1c03496](https://doi.org/10.1021/acsami.1c03496).
- 25 M. J. Al-Awady, P. J. Weldrick, M. J. Hardman, G. M. Greenway and V. N. Paunov, Amplified antimicrobial action of chlorhexidine encapsulated in PDAC-functionalized acrylate copolymer nanogel carriers, *Mater. Chem. Front.*, 2018, **2**, 2032–2044, DOI: [10.1039/c8qm00343b](https://doi.org/10.1039/c8qm00343b).
- 26 P. J. Weldrick, S. San and V. N. Paunov, Advanced Alcalase-Coated Clindamycin-Loaded Carbopol Nanogels for





- Removal of Persistent Bacterial Biofilms, *ACS Appl. Nano Mater.*, 2021, **4**, 1187–1201, DOI: [10.1021/acsnm.0c02810](https://doi.org/10.1021/acsnm.0c02810).
- 27 P. J. Weldrick, M. J. Hardman and V. N. Paunov, Smart active antibiotic nanocarriers with protease surface functionality can overcome biofilms of resistant bacteria, *Mater. Chem. Front.*, 2021, **5**, 961–972, DOI: [10.1039/DOQM00874E](https://doi.org/10.1039/DOQM00874E).
- 28 P. J. Weldrick, M. J. Hardman and V. N. Paunov, Super-Enhanced Removal of Fungal Biofilms by Protease-Functionalized Amphotericin B Nanocarriers, *Adv. Nanobiomed. Res.*, 2021, **1**, 2000027, DOI: [10.1002/anbr.20200002737](https://doi.org/10.1002/anbr.20200002737).
- 29 R. T. Chacko, J. Ventura, J. Zhuang and S. Thayumanavan, Polymer nanogels: a versatile nanoscopic drug delivery platform, *Adv. Drug Deliv. Rev.*, 2012, **64**, 836–851, DOI: [10.1016/j.addr.2012.02.002](https://doi.org/10.1016/j.addr.2012.02.002).
- 30 P. J. Weldrick, S. Iveson, M. J. Hardman and V. N. Paunov, Breathing New Life into Old Antibiotics: Overcoming Antibacterial Resistance by Antibiotic-Loaded Nanogel Carriers with Cationic Surface Functionality, *Nanoscale*, 2019, **11**, 10472–10485, DOI: [10.1039/C8NR10022E](https://doi.org/10.1039/C8NR10022E).
- 31 A. F. Halbus, T. S. Horozov and V. N. Paunov, Controlling the antimicrobial action of surface modified magnesium hydroxide nanoparticles, *Biomimetics*, 2019, **4**, 41, DOI: [10.3390/biomimetics4020041](https://doi.org/10.3390/biomimetics4020041).
- 32 S. S. M. Al-Obaidy, A. F. Halbus, G. M. Greenway and V. N. Paunov, Boosting the antimicrobial action of vancomycin formulated in shellac nanoparticles of dual-surface functionality, *J. Mater. Chem. B*, 2019, **7**, 3119–3133, DOI: [10.1039/c8tb03102a](https://doi.org/10.1039/c8tb03102a).
- 33 A. F. Halbus, T. S. Horozov and V. N. Paunov, Surface-Modified Zinc Oxide Nanoparticles for Antialgal and Antiyeast Applications, *ACS Appl. Nano Mater.*, 2020, **3**, 440–451, DOI: [10.1021/acsnm.9b02045](https://doi.org/10.1021/acsnm.9b02045).
- 34 M. J. Al-Awady, G. M. Greenway and V. N. Paunov, Nanotoxicity of polyelectrolyte-functionalized titania nanoparticles towards microalgae and yeast: Role of the particle concentration, size and surface charge, *RSC Adv.*, 2015, **5**, 37044–37059, DOI: [10.1039/c5ra05577f](https://doi.org/10.1039/c5ra05577f).
- 35 P. Henry, A. F. Halbus, Z. H. Athab and V. N. Paunov, Enhanced antimould action of surface modified copper oxide nanoparticles with phenylboronic acid surface functionality, *Biomimetics*, 2021, **6**, 1–16, DOI: [10.3390/biomimetics6010019](https://doi.org/10.3390/biomimetics6010019).
- 36 A. F. Halbus, T. S. Horozov and V. N. Paunov, Self-grafting copper oxide nanoparticles show a strong enhancement of their anti-algal and anti-yeast action, *Nanoscale Adv.*, 2019, **1**, 2323–2336, DOI: [10.1039/c9na00099b](https://doi.org/10.1039/c9na00099b).
- 37 A. F. Halbus, T. S. Horozov and V. N. Paunov, Strongly Enhanced Antibacterial Action of Copper Oxide Nanoparticles with Boronic Acid Surface Functionality, *ACS Appl. Mater. Interf.*, 2019, **11**, 12232–12243, DOI: [10.1021/acsnm.8b21862](https://doi.org/10.1021/acsnm.8b21862).
- 38 A. F. Halbus, T. S. Horozov and V. N. Paunov, “Ghost” Silica Nanoparticles of “host”-Inherited Antibacterial Action, *ACS Appl. Mater. Interf.*, 2019, **11**, 38519–38530, DOI: [10.1021/acsnm.9b14403](https://doi.org/10.1021/acsnm.9b14403).
- 39 A. F. Halbus, T. S. Horozov and V. N. Paunov, Colloid particle formulations for antimicrobial applications, *Adv. Colloid Interface Sci.*, 2017, **249**, 134–148, DOI: [10.1016/j.cis.2017.05.012](https://doi.org/10.1016/j.cis.2017.05.012).
- 40 S. S. M. Al-Obaidy, G. M. Greenway and V. N. Paunov, Dual-functionalised shellac nanocarriers give a super-boost of the antimicrobial action of berberine, *Nanoscale Adv.*, 2019, **1**, 858–872, DOI: [10.1039/c8na00121a](https://doi.org/10.1039/c8na00121a).
- 41 P. J. Weldrick, M. J. Hardman and V. N. Paunov, Enhanced Clearing of Wound-Related Pathogenic Bacterial Biofilms Using Protease-Functionalized Antibiotic Nanocarriers, *ACS Appl. Mater. Interf.*, 2019, **11**, 43902–43919, DOI: [10.1021/acsnm.9b16119](https://doi.org/10.1021/acsnm.9b16119).
- 42 S. S. M. Al-Obaidy, G. M. Greenway and V. N. Paunov, Enhanced Antimicrobial Action of Chlorhexidine Loaded in Shellac Nanoparticles with Cationic Surface Functionality, *Pharmaceutics*, 2021, **13**, 1389.1-15, DOI: [10.3390/pharmaceutics13091389](https://doi.org/10.3390/pharmaceutics13091389).
- 43 B. W. Filby, P. J. Weldrick and V. N. Paunov, Overcoming Beta-Lactamase-Based Antimicrobial Resistance by Nanocarrier-Loaded Clavulanic Acid and Antibiotic Cotreatments, *ACS Appl. Bio Mater.*, 2022, **5**, 3826–3840, DOI: [10.1021/acsnm.2c00369](https://doi.org/10.1021/acsnm.2c00369).
- 44 A. Wang, P. J. Weldrick, L. A. Madden and V. N. Paunov, Enhanced clearing of Candida biofilms on a 3D urothelial cell in vitro model using lysozyme-functionalized fluconazole-loaded shellac nanoparticles, *Biomater. Sci.*, 2021, **9**, 6927–6939, DOI: [10.1039/D1BM01035B](https://doi.org/10.1039/D1BM01035B).
- 45 P. J. Weldrick, A. Wang, A. F. Halbus and V. N. Paunov, Emerging nanotechnologies for targeting antimicrobial resistance, *Nanoscale*, 2022, **14**, 4018–4041, DOI: [10.1039/D1NR08157H](https://doi.org/10.1039/D1NR08157H).
- 46 E. O. Asare, E. A. Mun, E. Marsili and V. N. Paunov, Nanotechnologies for control of pathogenic microbial biofilms, *J. Mater. Chem. B*, 2022, **10**, 5129–5153, DOI: [10.1039/D2TB00233G](https://doi.org/10.1039/D2TB00233G).

